SINERGI Vol. 28, No. 3, October 2024: 461-472
http://publikasi.mercubuana.ac.id/index.php/sinergi
http://doi.org/10.22441/sinergi.2024.3.003

Fourier representation of geometrical imperfection for probabilistic buckling analysis

Pariatmono Sukamdo[1,*], Tuti Oktavia[1], Resmi Bestari Muin[1], Budianto Ontowirjo[2], Mohammad Ihsan[2], Sang Toga Sitompul[1]
[1]Department of Civil Engineering, Faculty of Engineering, Universitas Mercu Buana, Indonesia
[2]Department of Civil Engineering, Faculty of Engineering and Computer Science, Bakrie University, Indonesia

Abstract
This research studies the first part of the failure of a compression member structure due to buckling. This unstable equilibrium collapse, exposes brittle failure which occurs suddenly and therefore should be avoided wherever possible. Unavoidable geometric imperfections due to structural fabrication, will weaken the structure against buckling. The behavior of bar under compression will be closely examined by taking a set of geometric imperfection data synthesized from previously available from the measurement of conical shells. Therefore, the two-dimensional surface imperfection is converted into several one-dimensional imperfection with some probability properties. In order to obtain a comparison tool for different type of imperfections, Fourier analysis is used to convert the imperfection into coefficients of trigonometric function. By examining the coefficients, geometric imperfection patterns introduced by a certain fabrication process are able to be identified. The study successfully demonstrates the applicability of Fourier analysis in representing inherent geometric imperfections as an initial step for conducting probabilistic buckling analysis. Fourier analysis has shown its capability to simultaneously characterize imperfections in two crucial parameters - the magnitude and configuration of the imperfection.

Keywords:
Buckling Analysis;
Fourier Series;
Geometric Imperfection;
Probabilistic;

Article History:
Received: August 29, 2023
Revised: February 16, 2024
Accepted: March 24, 2024
Published: October 2, 2024

Corresponding Author:
Pariatmono Sukamdo
Civil Engineering Department, Universitas Mercu Buana, Indonesia
Email:
pariatmono@mercubuana.ac.id

INTRODUCTION

Concrete and steel are widely used materials in the construction industry. Concrete is favored for its versatility, durability, and cost-effectiveness [1]. Steel, on the other hand, is highly popular due to its durability, strength, and affordability [2]. As the most commonly used metal in construction, steel is also recognized for its eco-friendly nature as it is the most recycled material worldwide.

It is not known with certainty how much concrete is produced worldwide, but the total production of cement (which is the main component of concrete) worldwide will reach 2 billion tons in 2022 [3]. As for steel, production reaches 1,879 million tons [4].

The modulus of elasticity of steel is approximately ten times higher than that of concrete, which contributes to its superior strength [5]. Steel poles/columns, therefore, tend to be slenderer compared to their concrete counterparts [6]. This characteristic allows steel structures to achieve excellent space efficiency while also offering enhanced esthetic appeal in comparison to concrete structures.

However, for slender structures that are subjected to compressive loads (such as columns) will be very susceptible to buckling, even though the column is in a state of equilibrium. As it is widely accepted, if the energy in a continuum (a column for example) can be expressed by E, then the equilibrium state can be expressed as a minimum (potential) energy [7], or

$$\frac{dE}{dv} = 0 \qquad (1)$$

provided that

$$\frac{d^2E}{dv^2} > 0 \qquad (2)$$

In (1) and (2), E is energy stored in a continuum due to applied loads and v is deformation parameter of the continuum. If the condition in Eq. (2) is not met, i.e.,

$$\frac{d^2E}{dv^2} < 0 \qquad (3)$$

then we still have equilibrium state but an unstable one [8]. "Unstable equilibrium is a condition in which displacement of a system from its equilibrium position results in a net force or torque in the same direction as the displacement from equilibrium. This means that the system will accelerate away from its original position at the slightest disturbance." [9].

Buckling is an unstable equilibrium phenomenon [10]. In structural engineering, buckling is the sudden change in shape (deformation) of a structural component under load, such as the bowing of a column under compression. Buckling can occur in any structure that is loaded in compression, but it is most common in slender members, such as columns [11].

In order to systematically summarize the phenomenon mentioned above, Figure 1 contrasts the difference in behavior between a stocky and a slender column in responding to compressive load. It should be noted that the collapse of a structure due to buckling is a sudden and brittle failure [12]. The collapse is sudden because the buckling load is typically much lower than the yield strength of the material. This means that the member does not have time to deform plastically before it collapses. The collapse is also brittle because there is no warning before it happens. The member may be perfectly fine one moment and then collapse the next. Hence, the instability equilibrium in the form of buckling should be avoided.

This article takes a closer look at slender columns. As previously mentioned, the compressive force on a slender column will cause the column to buckle, which is a phenomenon categorized as unstable equilibrium. Mathematically, buckling events belong to eigenvalue problems. In the eigenvalue problem, each eigenvalue has an eigenvector. Physically, the eigenvalues are the loads that make the structure buckles, while the eigenvectors are the shape of the structure when it buckles [13].

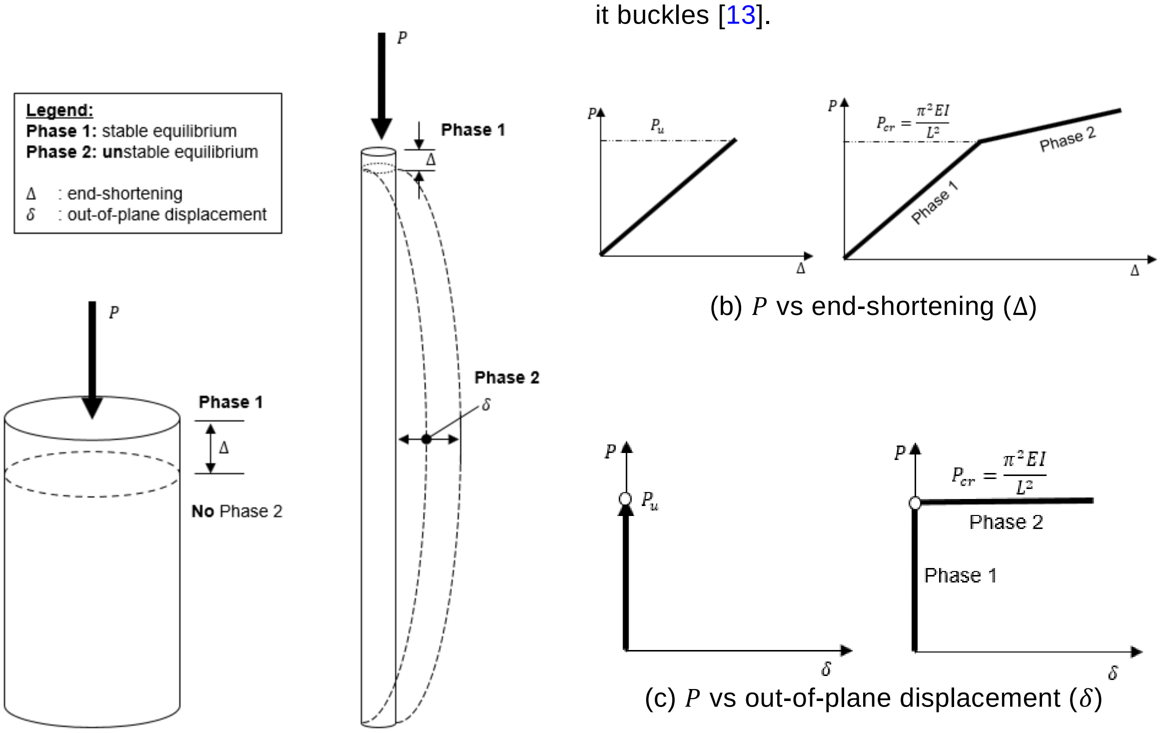

(b) P vs end-shortening (Δ)

(c) P vs out-of-plane displacement (δ)

(a) Structure Behavior

Figure 1. The Different Behavior for Stocky Column (left) and Slender Column (right) in Responding to Compressive Force

For a pin-ended slender column under compression, the formulated eigenvalue problem yields the following eigenvalues [14],

$$P = \frac{n^2\pi^2 EI}{L^2} \qquad (4)$$

In this equation, E, I and L are modulus elasticity, moment of inertia and length of the column, respectively and P is the eigenvalue aor buckling load. Setting $n = 1$, then the first eigenvalue is obtained which is the lowest buckling load. By taking $n = 2, 3, \cdots$, the second, the third and so forth will be obtained.

On the other hand, the eigenvectors or buckling mode corresponds to those buckling loads are shown in Figure 2.

The buckling loads expressed in (4) and their corresponding buckling modes in Figure 2 are related to a perfect column with no geometrical imperfection. For column with some geometric imperfection the buckling loads, i.e. the capacity of slender column to resist axial compression will be reduced [13]. Figure 3 illustrates the drop of column capacity with the presence of geometrical imperfection.

Apart from the amplitude of the imperfection, it can be easily understood that the reduction of the column capacity will be more pronounced if the form of the imperfection geometry is similar to buckling modes [14]. Therefore, a representation is needed to measure geometric imperfections based on two aspects at once, namely the amplitude and shape of the imperfections. This requirement can be met by using a Fourier Series which can decompose a series of numbers into the sum of trigonometric functions multiplied by a series of coefficients. As we all know, a periodic function $F(t)$ can be represented by the following Fourier Series [15].

$$F(t) = a_0 + \sum_{n=1}^{\infty} (a_n \cos n\Omega t + b_n \sin n\Omega t) \qquad (5)$$

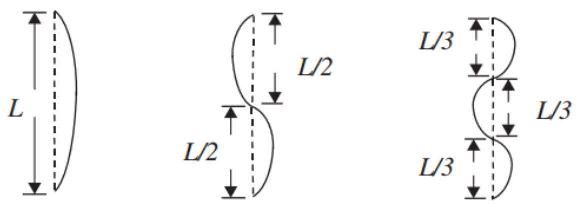

(a) (b) (c)

Figure 2. The First (a), the Second (b) and the Third (c) Buckling Modes of a Pin-ended Column under Compression (taken from [13])

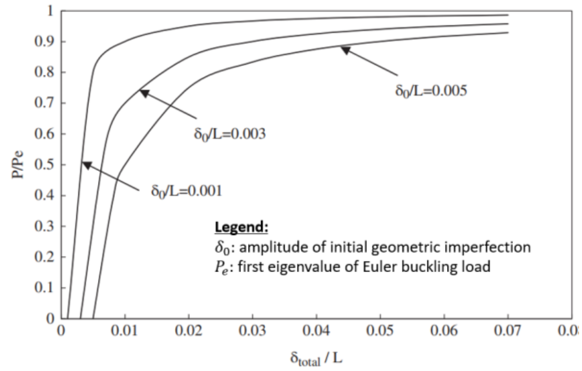

Figure 3. The reduction of slender column capacity in resisting axial compression with the presence of initial geometrical imperfection (adapted from [13])

In expression (5), a_0, a_1, $\cdots$, a_n and b_1, b_2, $\cdots$, b_n are called Fourier coefficient and ω is the frequency. The coefficients can be determine using:

$$a_0 = \frac{1}{T}\int_{t_1}^{t_1+T} F(t)\,dt$$

$$a_n = \frac{2}{T}\int_{t_1}^{t_1+T} F(t)\cos n\Omega t\,dt$$

$$= \frac{2}{T}\int_{t_1}^{t_1+T} F(t)\cos\frac{2n\pi}{T}t\,dt \qquad (6)$$

$$b_n = \frac{2}{T}\int_{t_1}^{t_1+T} F(t)\sin n\Omega t\,dt$$

$$= \frac{2}{T}\int_{t_1}^{t_1+T} F(t)\sin\frac{2n\pi}{T}t\,dt$$

As can be seen in (5), the Fourier coefficients show how dominant the term is in the overall Fourier representation. A coefficient which has a large value indicates that the term is dominant and therefore, geometric imperfections are also dominated by the number of waves associated with that term. In (5), for example, if the second term $(a_1 \cos \Omega t)$ and the fourth term $(a_2\, cos\, 2\Omega t)$ are taken, and supposed $a_1 > a_2$, then second term is more dominant than the fourth.

Furthermore, as the second has one full wave over the period and the fourth has two full waves, then it can be stated that the shape of geometrical imperfection is dominated by a single full wave. It also should be noted that if the Fourier series is used to express geometrical imperfections, then the coefficients of the Fourier series will demonstrate the amplitude of the imperfections, while the trigonometric functions will reflect the shape of the imperfections.

Meanwhile, the geometric imperfection is naturally not periodic. Hence, Fourier transforms should be used which converts a function of time or space into a function of frequency [16]. One-dimensional function of time (or space) variable $f(t)$ could be expressed as a linear combination of an infinite number of harmonic contributions [17].

$$f(t) = \frac{1}{\pi}\left[\int_0^\infty A(k)\cos kt\,dt + \int_0^\infty B(k)\sin kt\,dt\right] \quad (7)$$

The weighting factors that determine the significance of the various angular spatial frequency (k) contributions, that is $A(k)$ and $B(k)$, are the Fourier cosine and sine transforms of $f(t)$ given by

$$A(k) = \int_{-\infty}^{+\infty} f(t)\cos kt\,dt \quad (8)$$

and

$$B(k) = \int_{-\infty}^{+\infty} f(t')\sin kt'\,dt \quad (9)$$

Both equations can then be used to calculate Fourier coefficients of the unavoidable geometric imperfections.

METHOD

The world is not a place for something perfect. There is always imperfection in all objects. Likewise, in the manufacture of steel columns. The impacts of imperfections are identified in at least three aspects. Firstly, imperfection will reduce compressive capacity: Imperfections act as initiation points for buckling, where the column bends under load. Slender columns have less material to resist this bending, leading to a more significant decrease in capacity. Secondly, imperfection will induce eccentric loading: Even minor imperfections can cause the applied load to act off-center, further amplifying the bending effect. Thirdly, imperfection initiates unpredictable behavior: The exact impact of imperfections is difficult to predict due to their complex shapes and variations.

The slender the column is, the more likely geometric imperfections will occur which will result in, as previously mentioned, a decrease in the column's capacity to withstand compressive forces. This research is mostly carried out quantitatively. As mentioned earlier, geometry imperfections that inevitably occur due to fabrication, with Fourier analysis, are broken down into a summation of trigonometric functions with coefficients indicating the degree of dominance. In addition, performing Fourier analysis can also result in quantitively measure the similarity between the geometric imperfection to buckling modes.

The diagram in Figure 4 illustrates the comprehensive workflow undertaken to acquire proposals intended for inclusion in the pressure bar design standards, known as SNI in Indonesia. This process is driven by the understanding that structural members under compressive loads are significantly affected by geometric imperfections. Due to the diverse nature and intensity of these imperfections, the analysis for buckling load reduction necessitates running the model numerous times, as indicated in the lower right corner of Figure 4. Hence, it is imperative to employ rational statistical methods to minimize the number of iterations required while still achieving consistent results. This underscores the utilization of probabilistic buckling analysis techniques [18].

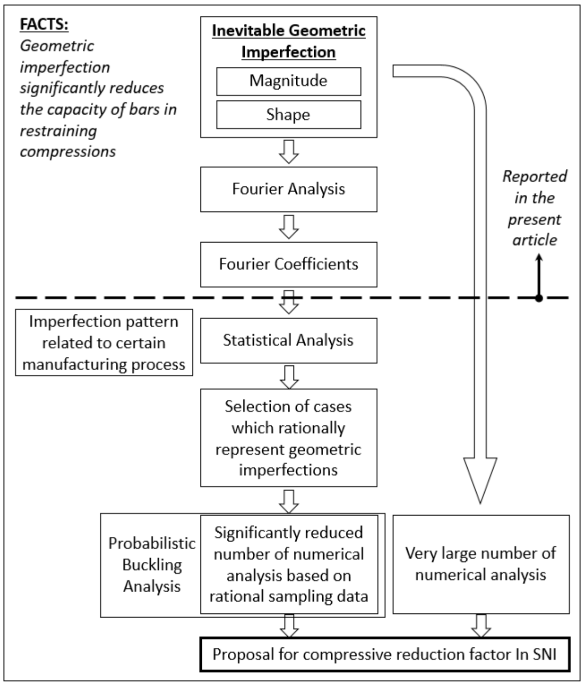

Figure 4. The systematic workflow of the present study

At least there are two ways of representing geometric imperfection for probabilistic analysis. Firstly, by using the equivalent load method. This approach involves defining the initial geometrical imperfections in analytical models by applying an approximate evaluation of the equivalent load [19]. Another approach in representing the geometric imperfection involves using Fourier analysis. This method decomposes the geometric imperfections into their constituent frequencies represented by Fourier series coefficients [20].

Both methods, the equivalent load method, and Fourier analysis, have their advantages and limitations. The equivalent load method is simpler and more straightforward to implement, as it involves adding a load to the structure to represent the geometric imperfection. However, it may not capture the full complexity of the imperfection, especially for complex shapes.

On the other hand, Fourier analysis allows for a more detailed representation of the geometric imperfection by decomposing it into a series of Fourier coefficients. This method can capture the spatial distribution of the imperfection more accurately, which is particularly useful for structures with complex geometries. However, it requires more computational resources and may be more challenging to implement [21]. The present work utilizes Fourier analysis, the second approach, to represent geometric imperfections.

It should be underlined that incorporating Fourier analysis in representing geometric imperfection is the first step towards the implementation of probabilistic techniques. Fourier analysis is a powerful tool for understanding and quantifying geometric imperfections in steel columns and their impact on buckling behavior. It works by treating the imperfection profile of a column as a wavy line and decomposing this function into a series of sine and cosine waves with different frequencies and amplitudes. Each wave has a corresponding coefficient that represents its strength or "dominance" within the overall imperfection profile. This method has been used to study the buckling behavior of steel columns, such as H-section columns and I-beams, providing analytical solutions to the generalized elastic thin-walled column buckling problem for different boundary conditions.

The geometric imperfections data are synthesized based on measurements that have been made on a shell surface [22]. The measurement results of geometric imperfections on a truncated conical shell are as shown in Figure 5 (a). This figure was taken as a part of shell buckling experimental program; hence a post buckling deformation measurement is also included but will not be utilized in the present analysis.

As can be seen, the imperfection readings consist of 14 rows. In each row, reading in the circumferential direction is taken. For the whole readings, the maximum imperfection was found to be -2.33 mm (outward) and +1.63 (inward).

Since the result of the geometry imperfection measurement experiment is only in the form of an image, it is necessary to digitize the image. For this purpose, the image is then processed using WebPlotDigitizer [23] which converts a curve image in Fig. 4 into pairs of x and y values.

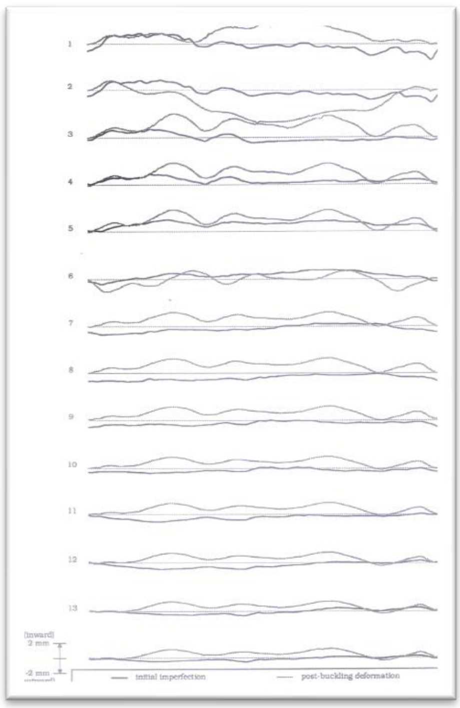

Figure 5 (a). Geometry Imperfections and Post-Bending Deformation of a Truncated Conical Shells, Row 1 to Row 14 (taken from [26])

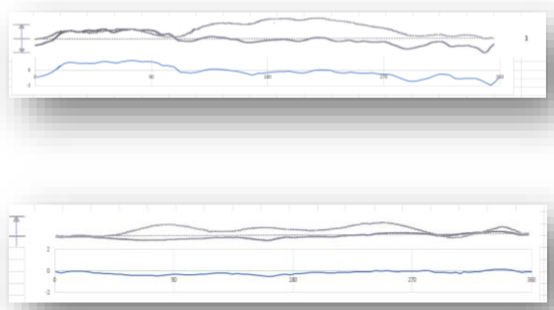

Figure 5 (b). Comparison of imperfections between measurement result (top, bold line) and result using [23] (bottom, blue line)

When contrasted, for example for row 1 and line 14, the comparison between the imperfections in Figure 5 (a) (above line) and the plot of the data (low line) looks like in Figure 5 (b). As can be seen, the use of WebPlotDigitizer [23] has successfully created reliable digital data from an image. The data resulted from running the software were then used for further representing geometric imperfection using Fourier Series. Therefore, it can be concluded that the limitation due to the inability to carry out direct measurements in the laboratory can be reduced by performing a synthesis of measurements that have been carried out by previous investigator.

RESULTS AND DISCUSSION

Figure 6 shows a portion of geometric imperfection data produced by running the WebPlotDigitizer program [23]. As mentioned earlier, this data is the readings from the shell surface imperfection which consists of 40 rows, each of which is a complete circle (360º). The first column of each row is the circular angle coordinates in degrees. In total there are about 3,800 readings were taken on the shell surface which should be sufficient to simulate the imperfection of compression members.

In order to produce a sufficient number of simulations for compressive bars, the imperfect surface was divided into 60 longitudinal strips, each at the same distance of 6 degrees. The geometric imperfection data for each bar is calculated by interpolation from the shell surface data in Figure 6.

Figure 7 shows some sample of geometric imperfection data on the rod which is a cut at positions 6, 12, 18, 354 and 360 degrees [24]. As discussed earlier, Figure 7 also confirms that the imperfections have a non-periodic nature, therefore coefficient of Fourier Transforms in form of (8) and (9) will be adopted. The computation resulted in coefficients which are presented in Figure 8 [24].

Figure 8 provides some of the results of calculating the Fourier coefficients. Columns show the Fourier coefficients, while rows show the cut position in degrees from 6º to 360º with 6º increments. The calculated coefficients are limited to 15 coefficients (from $A(0)$ to $A(7)$ and $B(0)$ to $B(7)$) because higher coefficients give very small value and can be ignored. Even in some cut positions, the values of $A(7)$ and $B(7)$ are already very small.

As demonstrated in Figure 9, the original imperfection curve of a bar (at a 6-degree cut) can be precisely reproduced by employing the corresponding Fourier coefficients. This implies that, instead of the full geometric imperfection shape, we can effectively encode and represent it using a series of these coefficients. A complete comparison of the geometrical imperfections of all the bars is presented in [25].

As mentioned previously, the circular coordinates are divided into intervals of 6 degrees, resulting in 60 bars with imperfect data. This number is sufficient to be used as a basis for statistical studies of geometric imperfections.

Row 1		Row 2		Row 39		Row 40	
1.76683	-0.89311	2.84E-14	-0.77043	0.782479	0.070726	1.53477	0.087954
5.786018	-0.72077	1.573835	-0.73937	4.954072	0.189864	5.95228	0.221532
9.805206	-0.46791	5.694018	-0.5599	8.905855	0.532084	9.661771	0.777824
13.97055	-0.17257	9.447962	-0.22786	12.84569	0.68526	13.37126	1.001752
19.52051	0.607039	14.9677	0.180185	16.86676	0.755287	17.57333	1.128219
341.2055	-1.05766	346.9367	-1.11432	331.9116	-0.32288	336.0666	-0.7364
345.2247	-1.24675	350.9653	-1.44315	335.9936	-0.37199	340.0802	-0.57975
349.0612	-1.60233	354.9939	-1.48871	340.0147	-0.3366	344.0937	-0.56745
352.8977	-1.9069	359.0225	-0.91885	344.0358	-0.28692	348.1073	-0.38414
356.0034	-1.51633	360.338	-0.68549	348.0568	-0.31604	352.1208	-0.34822
358.7438	-1.01099						

Figure 6. A portion of geometrical imperfection data resulted from [23]

Figure 7. Longitudinal imperfection of some section (6°, 12°, 18°, 354° and 360°)

Section (degree)	$A(0)$	$A(1)$	$B(1)$	$A(2)$	$B(2)$	$A(7)$	$B(7)$	ω
6	1.828	2.385	-2.464	0.5651	-3.277	-0.1123	0.5128	0.009992
12	6.334	7.645	-9.202	-1.296	-10.47	0.7209	0.4131	0.009221
18	2.69	3.694	-3.594	0.5803	-4.715	0.5248	0.5101	0.009293
24	-0.07957	0.4365	0.442	1.416	-0.107	0.07314	0.536	0.009617
30	4.977	7.198	-6.641	0.89	-8.565	0.4208	0.6468	0.009580
342	-0.7148	-1.626	0.8549	-0.6246	1.096			0.010870
348	-1.355	-2.512	1.564	-0.7095	1.994			0.010360
354	-2.349	-3.666	2.819	-0.5937	3.333			0.009845
360	-0.1767	-0.3242	-0.4779					0.057480
Average	**2.04456182**	**3.0852902**	**-2.60473**	**0.8121144**	**-3.585357**	**-0.026649589**	**0.352401143**	**0.012413**
Standard Deviation	**3.02877888**	**4.2236758**	**3.968082**	**1.000149**	**5.0753303**	**0.322542694**	**0.31860559**	**0.006592023**

Figure 8. The Fourier coefficient is obtained from the Fourier Transform equation, namely (8) and (9)

The Fourier series provides an excellent representation of actual geometric imperfections, allowing them to be replaced by a series of Fourier coefficients, such as $A(1)$, $A(2)$, $\cdots$, $A(7)$, $B(1)$, $B(2)$, $\cdots$, $B(7)$ and ω. These coefficients not only able to replace actual geometric imperfections but also indicate the dominant shape of a geometric imperfection. This is because each coefficient is a multiplier of trigonometric terms with clear periods and waveforms.

The coefficients $A(1)$, $A(2)$, $\cdots$, for example, is a multiplier of the term $\cos\omega x$, $\cos 2\omega x$, $\cdots$. Meanwhile the terms $\cos\omega x$, $\cos 2\omega x$, $\cdots$.themselves represent geometric functions that form one, two, etc., waves along the bar. Therefore, if $A(1)$ is bigger than $A(2)$, for example, then the imperfection is more dominated by a single cosine wave.

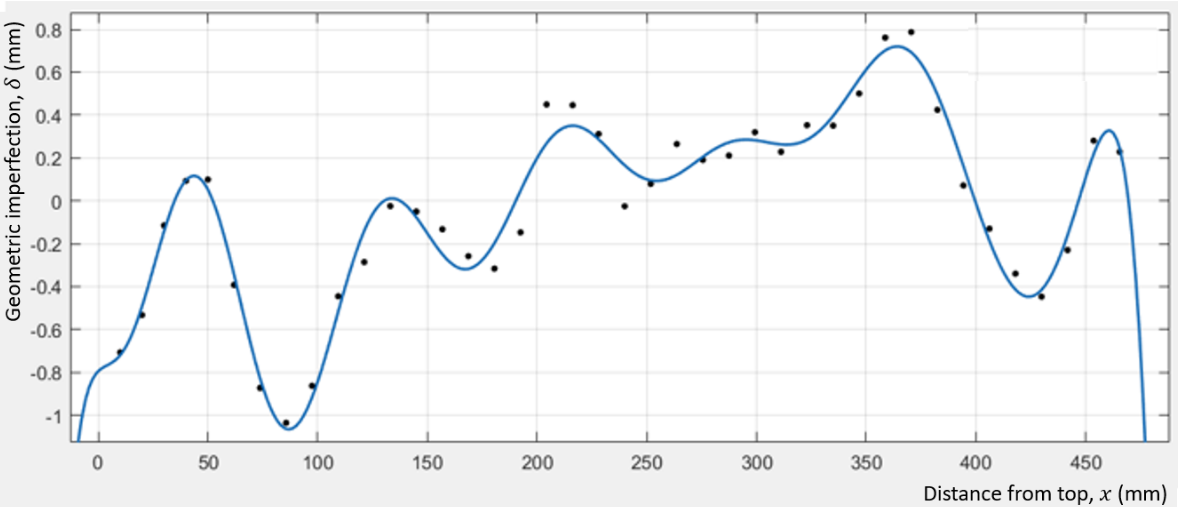

Figure 9. Comparison between the original imperfection (the dots) and the one formed based on the obtained Fourier coefficients (blue curve)

Figure 10 displays the Fourier coefficient values obtained from the geometric imperfection data of Bar 6°. The figure shows that the absolute value of the largest coefficient is $B(2)$, indicating that the imperfection in Bar 6° is dominated by two sine waves.

The complete calculation of Fourier coefficients for other bars are presented in [21]. As previously mentioned, the direction of the circumference of the shell surface is divided into 60, resulting in 60 bars, each with their own size and shape of the geometric imperfection. These imperfections are then decomposed into Fourier coefficients, resulting in 15 coefficients (namely $A(1), A(2), \cdots, A(7), B(1), B(2), \cdots, B(7)$) for each bar.

The large numbers of calculated Fourier coefficients enable the execution of statistical analysis to determine the distribution behavior of these coefficients. This is particularly significant as all bars are manufactured in the same manner at the factory. Therefore, it is reasonable to predict that all bars will exhibit similar patterns or tendencies of geometric imperfections. The statistical analysis of the Fourier coefficients is believed to be capable of identifying the size and shape of imperfections that are directly associated with the bar fabrication process in the factory.

Figure 11 demonstrates the value of the Fourier coefficient $A(1)$ for 60 bars. As previously mentioned, coefficient $A(1)$ is associated with geometric imperfections in the form of a cosine wave. The diversity in the values of $A(1)$ for different bars illustrates that not all bars have geometric imperfections dominated by a single cosine waveform. In fact, some bars have very small $A(1)$ values (for example, bar $102°$ to $120°$), indicating that the geometric imperfections for these bars do not contain a cosine waveform.

The average and standard deviation of the Fourier coefficient $A(1)$ for the 60 bars can be calculated to reflect how the Fourier coefficients are related to the geometric imperfections arising in the manufacturing process at the factory. For coefficient $A(1)$, the average obtained is 3.09 with a standard deviation of 4.19. These statistical characteristics provide insights into the nature of the geometric imperfections and their consistency across the manufactured bars.

The comprehensive outcomes of the statistical property calculations, presented in Figure 12, reveal a lack of discernible patterns in the average and standard deviation values. Notably, the standard deviation consistently surpasses the average across all coefficients, underscoring the fluctuating nature of the Fourier coefficients. This variability is attributed to the geometric imperfection data sourced from the shell surface.

The distinct processes involved in manufacturing shell surfaces and bars contribute to the imprecision when synthesizing imperfection data for compression bars from shell surface scans. Despite this, the analytical framework outlined in the study is anticipated to be applicable in scenarios where precise data on geometrical imperfections in compression members can be procured.

The methodology for representing geometric imperfections through a Fourier series is inherently significant. As previously elucidated, employing the Fourier series not only quantifies the magnitude of imperfections but also characterizes their form.

The magnitude and configuration of these imperfections play pivotal roles in determining the extent to which the load-carrying capacity of a bar diminishes under compression. Consequently, design regulations for compressed bars typically specify a factor that reduces the bar's capacity when subjected to compressive forces. The efficacy of this reduction factor is contingent on the consideration of geometric imperfections. Unfortunately, in the design standards for bars in Indonesia, specifically under SNI, encompassing both hot-rolled [26] and cold-rolled [27] categories, there is an absence of provisions addressing these imperfections.

The procedure discussed in this paper for expressing geometric imperfections using Fourier coefficients, followed by efforts to obtain statistical characteristics of these coefficients, enables the probabilistic buckling analysis of compressed members to be performed. This approach aims to obtain a reasonable reduction factor for the compression member capacity. Thus, a proposal can be made that SNI for designing steel structures in Indonesia, especially for designing compression members, can contain this reduction factor.

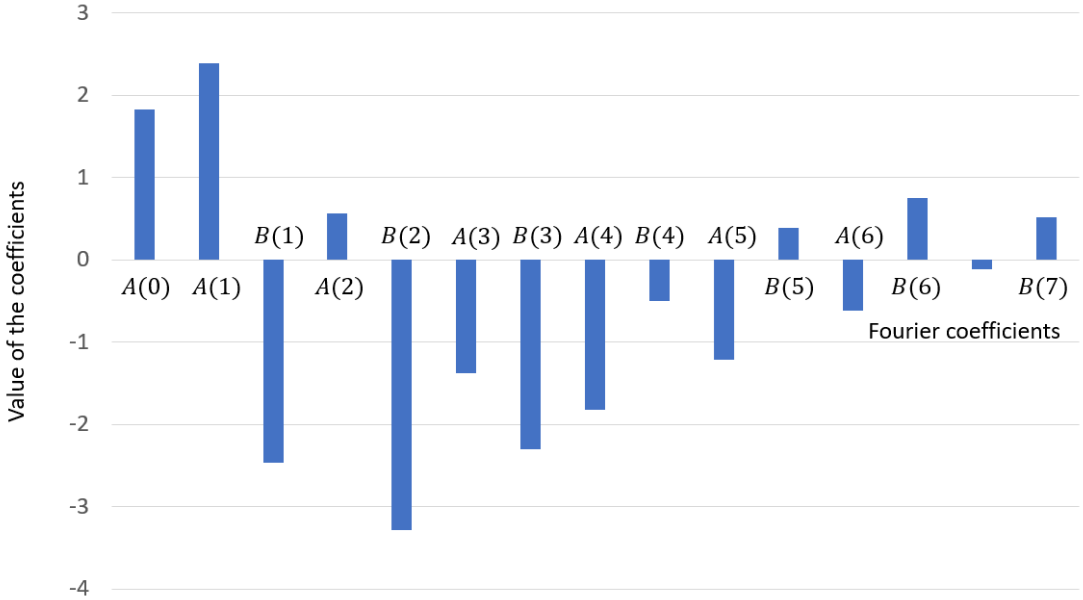

Figure 10. The value of Fourier coefficient of 6^0-bar

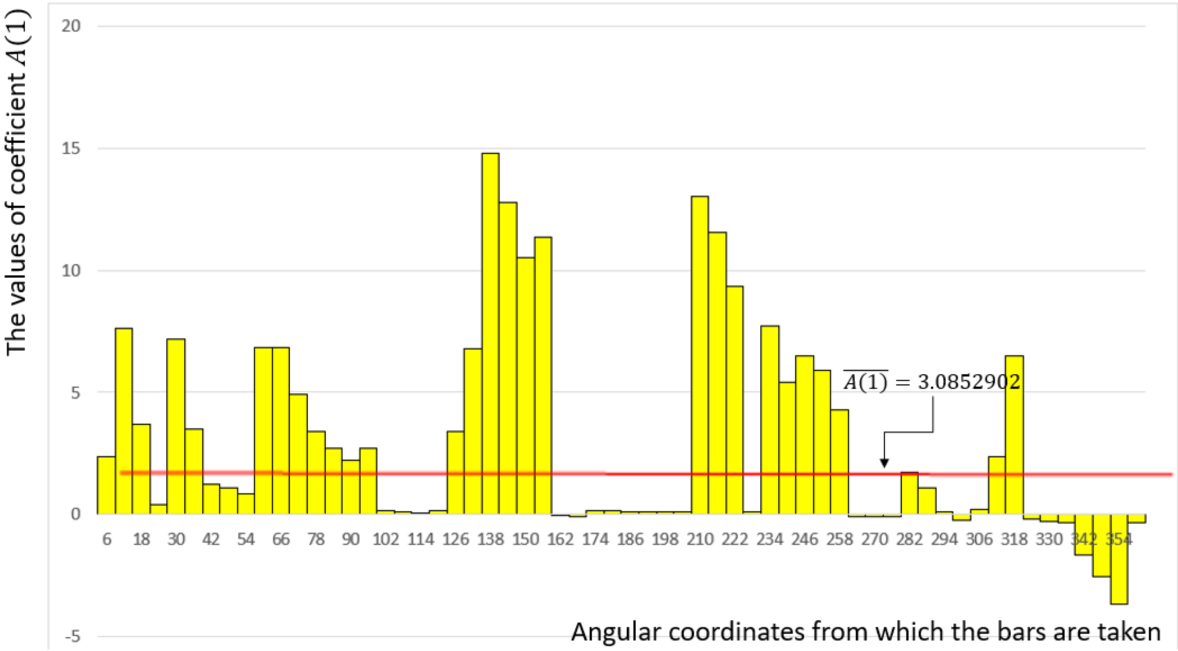

Figure 11. The value of $A(1)$ coefficients for various bars

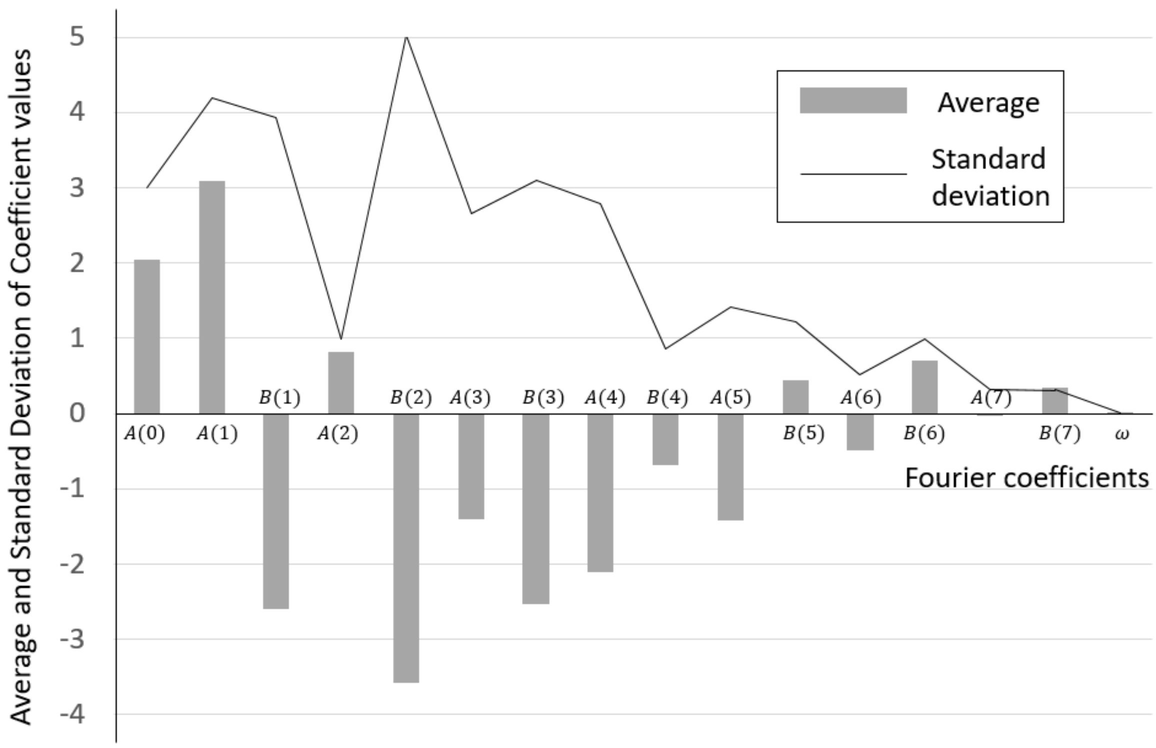

Figure 12. The mean and standard deviation of each Fourier coefficient

CONCLUSION

The article explains how to use Fourier series to represent geometric imperfections in steel structures. In terms of material properties, steel is known to be strong in resisting both tensile and compressive loads. However, structurally, compressive components are weaker than tensile components due to the presence of buckling phenomenon. Buckling is an unstable state in a compressive structure even though the forces acting on it are balanced. Geometric imperfections, such as those that occur due to the manufacturing process, can significantly reduce the compression capacity when they reach the buckling state. Both the size and shape of the imperfection greatly influence the reduction in the compression capacity of the structure. Fourier series can be used to quantitatively measure the similarity between imperfections and buckling modes.

The current design regulations for compression members in Indonesia only consider the magnitude of geometric imperfections and not their shape. This can lead to inaccurate designs. To address this, the article suggests incorporating the Fourier series method to represent both the magnitude and shape of these imperfections. This allows for a more accurate statistical analysis of their impact on compression members.

By understanding the statistical patterns of imperfections, engineers can utilize a probabilistic approach to analyze buckling loads. This leads to more reliable designs and facilitates the implementation of reduction factors in building regulations.

The article acknowledges the lack of data on steel bar imperfections in Indonesia but proposes using existing data from other sources as a starting point for developing the processing procedure. Further data collection is necessary for a more precise understanding of the local manufacturing case. The probabilistic buckling analysis of bars under compression is beyond the scope of this paper.

ACKNOWLEDGMENT

This research was funded by Universitas Mercu Buana. and Bakrie University fully supported the activity. In addition, we thank our students and colleagues from both universities who provided insight and expertise that greatly assisted the research.

REFERENCES

[1] D. M. Benghida, “Concrete as a Sustainable Construction Materials”, *Key Engineering Materials*, vol. 744, pp 196-200, 2017, doi: 10.4028/www.scientific.net/KEM.744.196

[2] P. Gatheeshgar, K. Poologanathan, S. Gunalan, I. Shyha, P. Sherlock, H. Rajanayagam, B. Nagaratnam, “Development of affordable steel-framed modular building for emergency situations (Covid-19)”, *Structures*, vol. 31, pp. 862-875, 2021, doi: 10.1016/j.istruc.2021.02.004.

[3] N. Tkachenko, K. Tang, M. McCarten, S. Reece, D. Kampmann, C. Hickey, M. Bayaraa, P. Foster, C. Layman, C. Rossi, K. Scott, D. Yoken, C. Christiaen, and B. Caldecott, “Global database of cement production assets and upstream suppliers,” *Scientific Data,* vol. 10, ID: 696, 2023, doi: 10.1038/s41597-023-02599-w

[4] G. Lopez, J. Farfan, C. Breyer,”Trends in global steel industry: Evolutionary projections and defossilition pathways through power-to-steel”, *Journal of Cleaner Production,* vol. 375, ID: 134182, 2022, doi: 10.1016/j.jclepro.2022.134182,

[5] J. C. Kim and W. Y. Lim, “Prediction of compressive strength and elastic modulus for ultra-high-performance concrete”, *Construction and Building Materials*, vol. 363, ID: 129883, January 2023, doi: 10.1016/j.conbuildmat. 2022.129883.

[6] P. Lacki, A. Derlatka, and P. Kasza, “Comparison of steel-concrete composite column and steel column”, *Composite Structures*, vol. 202, pp. 82-88, 2022, doi: 10.1016/j.compstruct.2017.11.055

[7] X. Fan, H. Chen, Y. Liu, and W. Lv, 2014, “Lifting Point Optimization of Large Steel Trus on the Principle of Minimum Potential Energy”, *Advanced Materials Research*, vol. 919-921, pp 158-163, doi: 10.4028/ www.scientific.net/amr.919-921.158

[8] W. Huang, Y. Zhang, T. Yu and M. Liu, “Bifurcations and Stability Analysis of Elastic Slender Structures Using Static Discrete Elastic Rods Method,” *Journal of Applied Mechanics*, vol. 90, no. 9, ID: 094501, 6 pages, Paper No: JAM-23-1100, Sep 2023, doi: 10.1115/1.4062533

[9] A. Dalklint, M. Wallin, D.A. Tortorelli, “Structural Stability and Artificial Buckilng Modes in Topology Optimization”, *Journal of Structural and Multidisciplinary Optimization*, vol. 64, pp. 1751-1763, October 2021, doi: 10.1007/s00158-021-03012-z

[10] M. Nistor, R. Wiebe, I. Stanciulescu, “Relationship between Euler buckling and unstable equilibria of buckled beams,” *International Journal of Non-Linear Mechanics*, vol. 95, pp. 151-161, October 2017, doi: 10.1016/j.ijnonlinmec.2017.06. 016

[11] F. Sinur, A. Zizza, U. Kuhlmann, D. Beg, “Buckling interaction of slender plates - Experimental and numerical investigations,” *Thin-Walled Structures*, vol. 61, pp. 121-131, December 2012, doi: 10.1016/j.tws.2012.03. 024

[12] J. R. Gladden, N. Z. Handzy, A. Belmonte, and E. Villermaux, “Dynamic Buckling and Fragmentation in Brittle Rods,” *Physical Review Letters,* vol. 94, ID: 035503, January 2005, doi: 10.1103/PhysRevLett.94.035503

[13] S. Jerath, “Structural Stability Theory and Practice – Buckling of Columns, Beams, Plates, and Shells”, Wiley, 2021

[14] S.A.M. Ghannadpour, B. Mohammadi, J. Fazilati, “Bending, buckling and vibration problems of nonlocal Euler beams using Ritz method,” *Composite Structures*, vol. 96, pp. 584-589, February 2013, doi: 10.1016/j.compstruct.2012.08.024

[15] E. Kreyzig, “Advanced Engineering Mathematics”, 10th Edition, John Wiley & Sons, 2011.

[16] C. Mateo, and J. A. Talavera, “Short-time Fourier transform with the window size fixed in the frequency domain,” *Digital Signal Processing*, vol. 77, pp. 13-2, 2018, doi: 10.1016/j.dsp.2017.11.003

[17] M. Latifi, F. Farhatnia, and M. Kadkhodaei, “Buckling analysis of rectangular functionally graded plates under various edge conditions using Fourier series expansion,” *European Journal of Mechanics - A/Solids*, vol. 41, pp 16-27, September–October 2013, doi: 10.1016/j.euromechsol.2013.01. 008

[18] D. De Domenico, G. Falsone, and D. Settineri, “Probabilistic buckling analysis of beam-column elements with geometric imperfections and various boundary conditions,” *Meccanica*, vol. 53, pp. 1001–1013, 2018, doi: 10.1007/s11012-017-0763-5

[19] G. Augusti, and S. Chiostrini, “A Simple Way to Represent Geometrical Imperfections by Means of an Equivalent Load,” *Mechanics of Structures and Machines*, vol. 20, no. 1, pp. 17-35, 1992, doi: 10.1080/ 08905459208905158

[20] M. A. Rendall, and K.J.R. Rasmussen, “Localized geometric imperfection analysis and modelling using the wavelet transform,” *Thin-Walled Structures*, vol. 96, pp. 202-219, November 2015, doi: 10.1016/j.tws.2015.08. 007

[21] W. Liu, K.J.R. Rasmussen, H. Zhang, Y. Xie, Q. Liu, and L. Dai, “Probabilistic study and numerical modelling of initial geometric imperfections for 3D steel frames in

advanced structural analysis," *Structures*, vol. 57, ID: 105190, 2023, doi: 10.1016/j.istruc.2023.105190.
[22] Pariatmono, "The Collapse of Conical Shells under Axial Compression", *PhD Thesis*, Department of Civil Engineering, Imperial College of Science, Technology and Medicine, London, UK, 1994
[23] A. Rohatgi, *WebPlotDigitizer version 4.3*, available from https://automeris.io/WebPlotDigitizer/download.html
[24] T. Octavia, Pariatmono, "Probabilistic Buckling Analysis of Compression Bar of Lightweight Steel", submitted to Jurnal Rekayasa Sipil (in Bahasa Indonesia), 2023
[25] T. Octavia, "Probabilistic Buckling Analysis for Cold-Formed Steel Bar", Post Graduate Thesis (in Bahasa Indonesia), 2023.
[26] BSN (Badan Standarisasi Nasional), SNI 1729:2015, "Specifications for structural steel buildings" (in Bahasa Indonesia), 2015
[27] BSN (Badan Standarisasi Nasional), SNI 7971:2013, "Cold Rolled Steel Structure" (in Bahasa Indonesia), 2013.